辐射防护及相关学科论文集

李德平　潘自强　胡遵素　等著

原子能出版社

图书在版编目(CIP)数据

辐射防护及相关学科论文集(SELECTED WORKS FOR RADIATION PROTECTION AND RELATED TOPICS)/李德平、潘自强、胡遵素等著 .—北京:原子能出版社,1996.10

ISBN 7-7022-1603-0

Ⅰ.辐… Ⅱ.李… Ⅲ.辐射防护-研究-文集 Ⅳ.R.142-53

中国版本图书馆 CIP 数据核字(96)第 17993 号

内 容 简 介

本文集选录了中国科学院院士、中国辐射防护研究院名誉院长李德平先生以及国内辐射防护界部分人士发表过的和未发表过的学术论文 70 余篇。这些论文涉及辐射防护、辐射物理、核电子学与探测技术、核安全与辐射安全、环境保护和辐射损伤与效应等领域,部分反映了国内该领域的科研活动与发展历程。在李德平院士从事辐射防护工作 42 年之际,组织出版本论文集是一次有益的回顾与总结。

本文集可供上述领域的广大科技工作者和有关大专院校师生阅读和参考。

原子能出版社出版发行

责任编辑:李 镁

封面设计:崔 彤 技术编辑:杨京蜀

社址:北京市海淀区阜成路 43 号 邮政编码:100037

原子能出版社 印刷厂印刷 新华书店经销

开本:787×1092 mm 1/16 印张 33.5 字数 840 千字

1996 年 10 月北京第一版 1996 年 10 月北京第一次印刷

印数:1—500

定价:(精)81.00 元

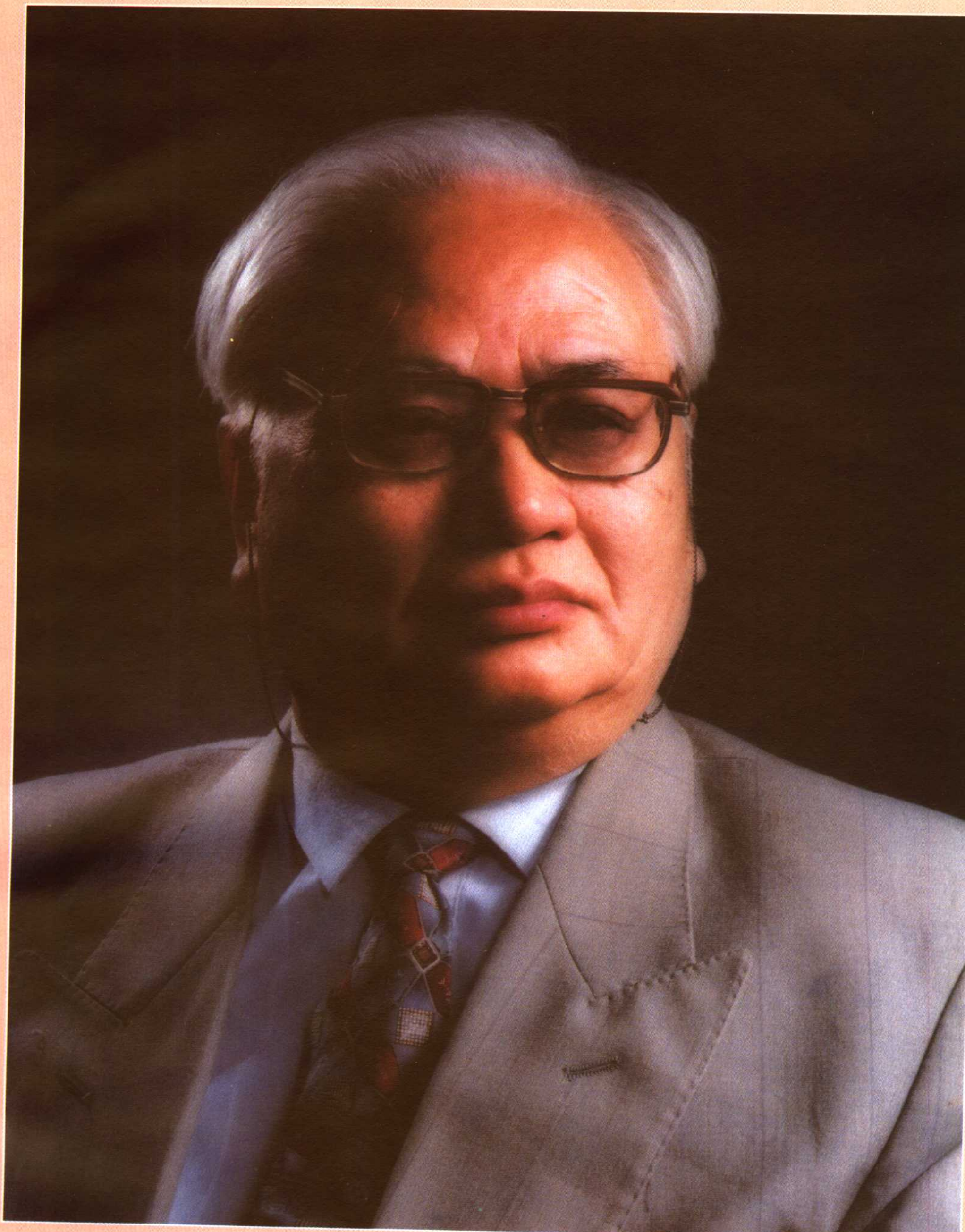

李德平院士近照(1995 年)

张建设 摄影

国际放射防护委员会(ICRP)主委员会全体委员在美国(1990 年)

国际原子能机构(IAEA)核安全咨询顾问组(INSAG)全体成员在维也纳(1992 年)

李德平院士与来自台湾地区的辐射防护专家翁宝山亲切交谈 (1993 年)

李德平院士与夫人王怀珍及外孙女在长岛(1992 年)

前　言

今年11月4日是我国著名的辐射物理、辐射防护与核安全专家、中国科学院院士、中国辐射防护研究院名誉院长、国际放射防护委员会(ICRP)主委员会委员李德平先生从事辐射防护工作42年和70寿辰。李德平先生不仅是我国核工业辐射防护学科的开创者和奠基人;而且,他的博大精深的学识,严谨的学风,以事业为己任的敬业精神和为人师表的高尚品德,感染并造就了我国核工业辐射防护系统一大批科研和技术骨干(包括以后调入其他有关单位的一些同志),他们中的许多人发表的第一篇或最主要的论文都倾注着李先生的智慧、关心和帮助。在庆贺李先生70寿辰之际,由中国核工业总公司安防环保卫生局、中国辐射防护研究院、中国辐射防护学会、中国原子能科学研究院保健物理部、国家环保局监督管理司辐射处和四川联合大学核技术应用研究所等单位联合组织征文、编纂本文集。这是对李先生诲人不倦、不惜以自己创造性思想之光点燃他人智慧之火的崇高精神的敬仰和回报;又表示我们将继续推进李先生关于加强学术交流的一贯主张,以繁荣辐射防护事业。

此次征文共征集到论文150多篇,由于篇幅所限,收入本文集70余篇。其中包括李德平先生过去没有公开发表的论文三篇;还包括部分著名专家早期在李德平先生指导下发表的有相当重要意义的论文或近期完成的新作。文集的内容涉及辐射防护、辐射物理、核电子学与探测技术、核安全与辐射安全、环境保护和辐射损伤与效应等,可供有关专业研究人员参考。

原子能出版社孙家辉、李盈安和韩国光编审参加了本论文集的审稿工作,特在此致以谢意。

《辐射防护及相关学科论文集》编委会

1996年9月

目　　录

A　辐射物理

B　保健物理

C　核电子学与探测技术

D　核安全与辐射安全

E　环境保护

F 辐射损伤与效应

G 其 他

A 辐射物理

PERFORMANCE AND OPTIMIZATION OF POTENTIAL ALPHA-ENERGY CONCENTRATION MEASUREMENT

Li Deping

(Institute of Radiation Protection, MNI P. O. Box 120, Taiyuan, Shanxi, P. R. China)

Abstract Some calculations were made to evaluate procedures for Rn daughters pontential alpha-energy concentration C_E measurements through filter sample counting, possible difference in counting efficiencies for different alphas have been taken into consideration. A method for selecting the time schedule for measurement with given total time, to minimize the dependence of the estimated C_E on the concentration ratios, is presented. It is found that two counts at selected times can eliminate this dependence.

Possible improvements with separate RaA counting, and the optimized time schedule for daughter concentrations measurements, have been preliminarily explored. Some slight improvement is gained by inserting a waiting time between the two counting intervals. Influence of change of concentrations or sampling rate during sampling is briefly discussed.

The potential α-energy concentration of Rn daughters in air is more directly connected with the hazards to person exposed to Rn and its daughters. This quantity is a weighted sum of the activity concentrations C_A, C_B, C_C of the three daughters RaA, RaB and RaC:

$$C_E = E_1C_A + E_2C_B + E_3C_C = 3.611C_A + 17.815C_B + 13.095C_C \text{(GeV/Bq)} \quad (1)$$

In field methods, the α-activity of daughters on a filter sample of the air is counted in an appropriate time interval after sampling. This count is another weighted sum of the concentrations

$$N = \eta_C v n \qquad n = (aa\eta_A/\eta_C + ac)C_A + bC_B + cC_C \quad (2)$$

here η_A, η_C are counting efficiencies for alphas from RaA and RaC, v volume sampled in unit time, a, b, c, aa, ac are constants determined by the time schedule adopted. Following the classical Kusnetz's method, approximate value of C_E is obtained by multiplying N with a constant k. This inevitably introduces an error of the method, whose magnitude depends on the range of possible concentration ratios $X(=C_B/B_A)$, $Y(=C_C/C_A)$ encountered. Various modifications have been proposed with a view to improve the accuracy or to reduce time. Such proposals had been reevaluated by us, and the general trends of performance and optimization of such methods have been studied.

On the X—Y plane, possible values of concentration ratios are enclosed in the curve representing the growth of daughters with Rn age and the straight line, joining its ends, since mixture of Rn of different ages can not go outside. As the ventilation rate is limited in practice, extreme points(e. g. with ventilation rate greater than 10 times per hour) can be excluded* as shown in fig. 1.

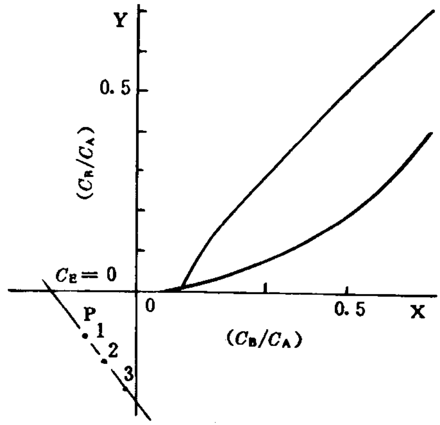

Fig. 1 Region of possible values of concentration ratios

If the straight lines $N=0$, $C_E=0$ meet at the point P (X_P, Y_P), then points on any straight line passing throught P

$$Y-Y_P=m\cdot(X-X_P)$$

where m is the slope, will give the same

$$C_E/n = (E_1 + E_2\cdot X + E_3\cdot Y)/(a + b\cdot X + c\cdot Y)$$
$$= (E_2 + m\cdot E_3)/(b + m\cdot c) \qquad (3)$$

And two such lines (with slopes m and m_T) touching the boundary of the concentration ratio region give the range of values of C_E/n. These slopes and the Rn age corresponding to the point of contact are shown in fig. 2. Now the trick of narrowing down the range of C_E/n lies in selecting P for small viewing angle substended by this region and keeping the angle between $C_E=0, n=0$ small (b/c near to $E_2/E_3=1.36$).

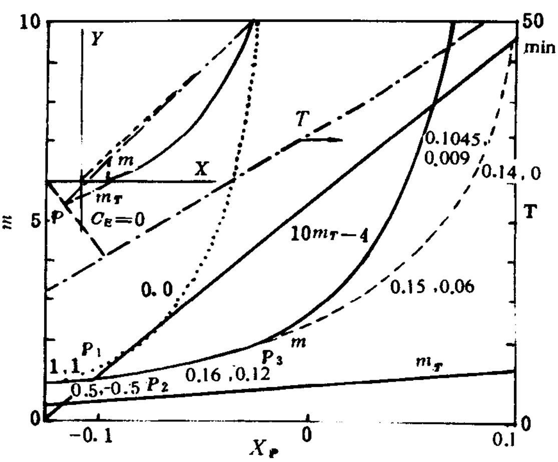

Fig. 2 Slopes m, m_T of bond lines passing P on $C_E=0$

It is convenient for general discussion to introduce an effective delay time T_D' which is the time between instantaneous sampling and counting that gives the same value of b/c. With non-overlapping sampling interval and counting interval of time t_s and t_m, and the time between the mid-points of each interval T_D, we can rewrite(2) into

$$n/\psi_s\psi_m=(aa'R+ac'-waa')C_A+b'C_B+c'C_C$$
$$T_D'=T_D+\Delta T_s+\Delta T_m$$
$$R=(\eta_A/\eta_C+w)\zeta_s\zeta_m \qquad (4)$$

---

* Extreme concentration ratios may occure down stream a near by strong local Rn source or when an efficient local recirculating filter is operated.

where $w=0.023525$, aa' to C' are corresponding coefficients for the effective delay time while ψ and ζ correction factors ΔT correction for finite t_s and t_m, as shown in fig. 3. Thus slope of the line $n=0$ is determined by T_D', while ζ depends on T_D' and R.

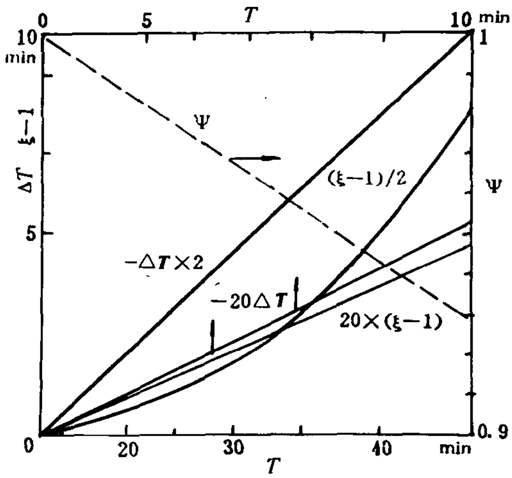

Fig. 3 Correction for finite sampling and counting times

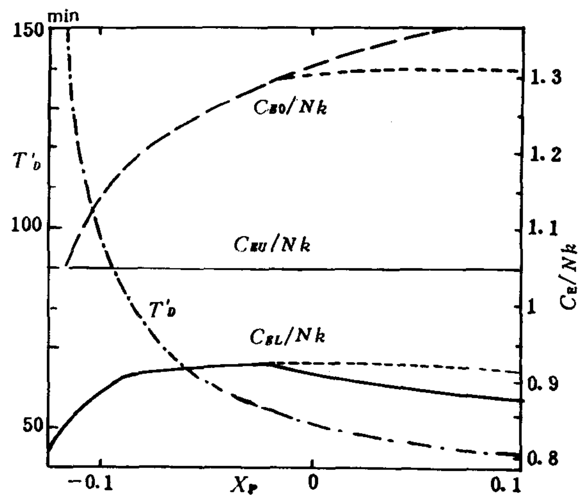

Fig. 4 C_E/Nk and effective delay time T_D' for Kusnets's method

For the Kusnetz's method, the term $aa'\ R$ is negligible, and the point P is nearly uniquely determined by T_D'. Relationships between T_D', C_E/Nk and X_p are shown in fig. 4. When T_D' increases from 45 min, the effect of increase of the angle between $C_E=0$ and $n=0$ is compansated by the decrease of viewing angle up to 83min. This is illustrated by the curve for C_{EL}/Nk, the lower branch corresponds to the extreme point $X=0.1045$, $Y=0.009$, it follows the same trends but T_D' longer than 50 min, is preferable. When the point 0, 0 is included, the upper bound of C_E will be significantly higher, this means undesirable underestimation and longer delay time, say 83 to 155 min., helps to reduce it.

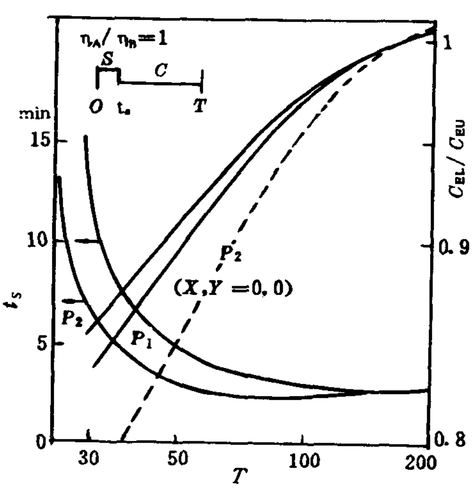

Fig. 5 Reduction of error with long counting and early starting

When we start counting early enough to catch sufficient RaA alpha counts to keep P at the optimun point P_2 $X=-0.08753$. (or P_1, $X=-0.11682$ when 0,0 is included), furhter reduction of error is possible with long time counting as shown in fig. 5 for $\eta_A/\eta_C=1$, 2.669min sampling followed by 160min, counting will eliminate this error completely.

For the rapid methods, the parameter R is very important. Since T_D' =33.19min. (i.e. b/c 1.36), for fixed P, increase of T_D' will decrease the angle between $C_E=0$ and $N=0$, and reduce the range of C_E/N; and optimun T_D' is determined by R and increases with R, as more time is needed for the RaA to decay to the required counting rate. Such trends are clearly shown in fig. 6 and fig. 7; in these figures C_{EU} to C_{EL} is the range of C_E under normal ventilation rate and C_{EU} corresponding to the extreme case $X, Y=0, 0$, the value of C_{EU}/Nk is assigned to be 1.1 through choice of k.

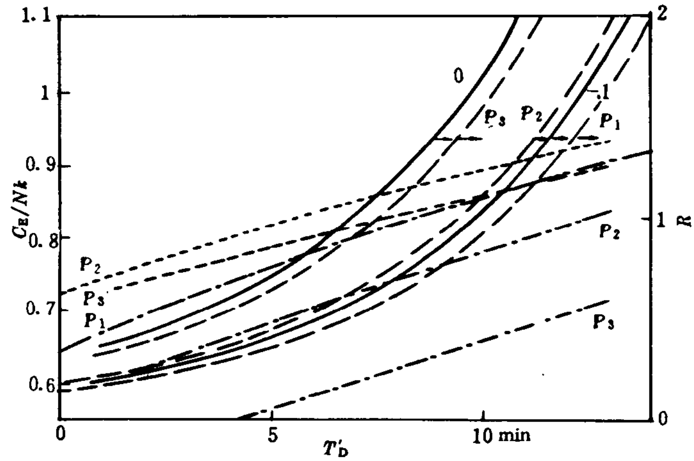

Fig. 6 R and C_E/Nk for rapid methods

— · — · — · C_{E0}/Nk

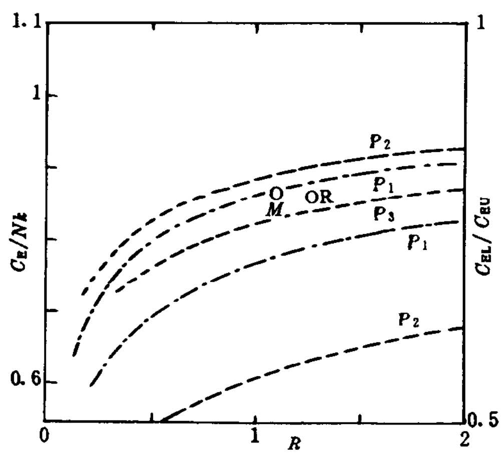

Fig. 7 Curve of C_E vs R circles indicate Markov's and Rolle's methods

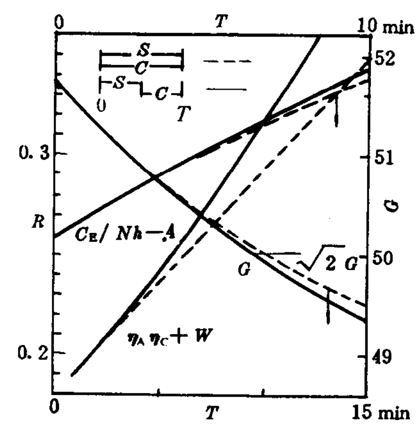

Fig. 8 Parameters for instant methods
G is proportional to counting fluctuations

R and C_E/Nk for the Rolle's and the Markov's methods are also indicated in fig. 7, they are near to the curve for P_1 (optimun including 0,0), yet leave some room for slight improvement: for instance, shorten T_D by 39 sec. C_E/Nk will increase from 0.859 to 0.881 and to 0.90 on the curve for P_2 with 99.5 sec. shortening.

It is possible to save time further, at the expanse of some increase of the range of C_E/Nk, through intentional reduction of η_A/η_C. To the extreme one gets various instant methods. For the measurement schemes illustrated in fig. 8, $T_D \doteq T/2$ when $t_s = t_m = T/2$, *and* $T_D' \doteq T/3$ when sample and count simultaneously with $t_s = t_m = T$, $t_s = t_m = T$, thus C_E/Nk can be read from the left end of the same curve in fig. 7. Exact values of C_E/Nk and the $\eta_A/\eta_C + w$ required are plotted in fig. 8, coefficient of variation of the estimated $C_E(Nk)$ is given through G in the figure with

$$CV = G/(\sqrt{Nk \cdot \eta_C v \cdot T}) \tag{5}$$

With $\eta_C = 0.35$, $v = 2$ l/min, $t = 5$min. CV due to counting statistics will be 17% at one tenth of the ICRP DACa.

It is also possible to combine two counts N_1, N_2 of the same sample at different time together as N, e.g. $N = r N_1 + N_2$. For the instant metoods, r is chosen for intersection P_2 and circumambulate the need of tailoring η_A/η_C when it is known. In most cases, η_A/η_C is higher than the value needed, and r is nagative; this increases T_D' with slight improvement in C_E/Nk, but the counting fluctuation increases enormously. Fig. 9 demonstrates these trends for the time schedule: half of the total time for sampling and counting and half for the second counting.

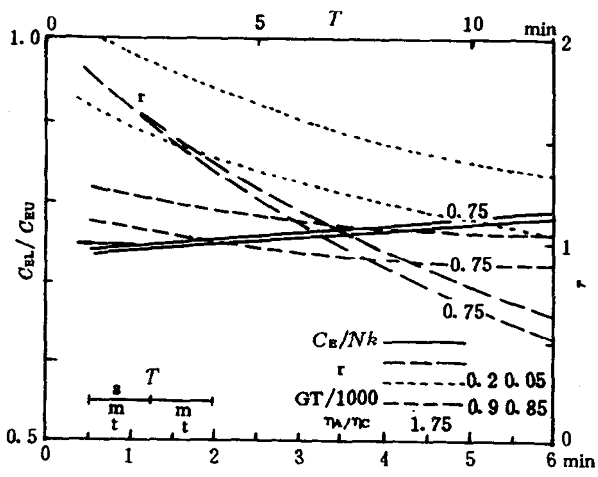

Fig. 9 Instant methods with two counting intervals

When we chose the second counting interval with T_D' arround 33 min, the error of the method will be drastically reduced or even eliminated; for example, $\eta_A/\eta_C = 1.0$—5min sampling and simutaneous counting 35.96—45.96 min second counting with $N = 0.21250\, N_1 + N_2$, and $\eta_A/\eta_C = 0.75$, 38.02—48.02 min second counting with $N = 0.27994 N_1 + N_2$.

When the measuring scheme makes the three straight lines $C_E = 0, N_1 = 0, N_2 = 0$ meet at the same point, choosing

$$r=(-b_2E_2-c_2E_3)/(b_1E_2-c_1E_3) \quad (6)$$

then C_E/N is a constant and independent of the concentration ratios X and Y, i. e. free from this error of the method.

For example, any rapid method with intersection at P_2 for routine monitoring, can be combined with the Kusnetz's method with delay time of 83. 3 min for some important data or when extreme ventilation conditions might have happened. Colinear mapping between the X,Y plane and the N_2/N_1, C_E/N_1 plane had been used to deal with pair of counts not exactly matched on P.

To count alphas from RaA and RaC separately with spectrometric method, one would provide more fluxibility in obtaining the effective η_A/η_C required. One possibility of utilizing this additional information is to narrow down the range of X and Y with the constraint, see equation (3). Typical performance is shown in fig. 10.

$$bX+cY=a a\eta_C/\eta_A-ac \quad (7)$$

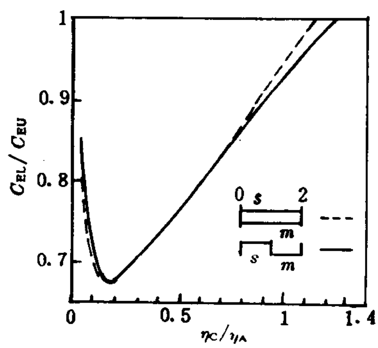

Fig. 10 Inprovement with known N_A

As to the measurement of the concentrations of the three daughters, some calculations have been made on the method counting separately N_A and N_C with spectrometric instruments in two counting intervals. N_A in the first interval gives C_A directly, and then C_B and C_C are solved from the two N_C counts. Optimization of the time schedule depends on the objective function aimed at, and the concentration ratio is also involved, and two levels of degree of equilibrium $X,Y=0.9, 0.85$ (H) and 0. 2, 0. 05 (L) are considered. To illustrate the trend we choose as the objective function some thing mid-way between the sum of variances and the sum of square of coefficients of variation of the daughters i. e.

$$OB=(\sigma_A^2+\sigma_B^2/X+\sigma_C^2/Y)/C_A^2 \quad (8)$$

it is only an index as correlations between estimated values are ignored. The time schedule thus optimized is shown in fig. 11, H is proportional to the objective function

$$OB=S/(60T\eta_C vEC) \quad (9)$$

where EC is the equvalent equibrium Rn concentration. When the time schedule shifts to that optimized for the other level, increase in S (shown with short vertical bars) is slight, so a schedule mid-way between these two would be appropriete for practical purpose. H for other indices, for the same schedule is shown in fig. 12 with the shifted curves in dotted lines.

It is interesting to note that a waiting time T_G between the two counting intervals can decrease the S (unfortunately, by less than 10%). As the effect of decrease of counts, hence the variances, is dominating at moderate T_G. Similar effects are observed for other plausible objective functions, as shown in fig. 13. On the other hand, waiting time between sampling and counting will increase H and should be minimized.

The assumption of constancy of the product v • concentration for all the three daughters, during sampling, taken for granted in most such works, have been examined. In most cases, 20% decrease during sampling will decrease the estimated C_E by a few percents even for pure RaA, and far less for higher X and Y. For concentration measurement, the situation is less happy, usually the error of concen trations and their ratios are less than 10%.

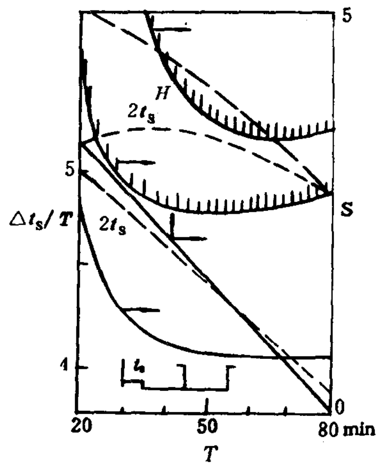

Fig. 11 Optimized time schedule for daughter conc. OBJ see equation (8)

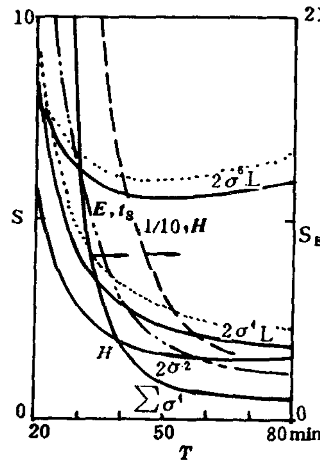

Fig. 12 S for other combinations of statistical error

APPENDIX

The counts corrected for counting efficiency and sampling rate are:

$$n_A = aaC_A$$

$$n_C = acC_A + bC_B + cC_C \qquad (A1)$$

where $\quad aa = f_1 \qquad c = f_3$

$$b = \frac{\lambda_3}{\lambda_3 - \lambda_2} \cdot (f_2 - f_3)$$

$$ac = \frac{\lambda_2}{\lambda_2 - \lambda_1} \times \frac{\lambda_3}{\lambda_3 - \lambda_1}(f_1 - f_3) + \frac{\lambda_2}{\lambda_1 - \lambda_3} \times \frac{\lambda_3}{\lambda_3 - \lambda_2}(f_2 - f_3)$$

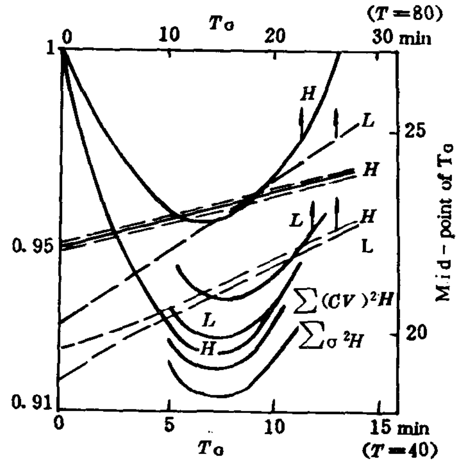

Fig. 13 Reduction of a with waiting time T_G t_s=40,10.43;80,15.55 min

For non-overlapping sampling time t_s, counting time t_m and the delay time between the mid-points of the two intervals T_D,

$$f_i = 4 \cdot \sinh(\lambda_i t_s/2) \cdot \sinh(\lambda_i t_m/2)\exp(-\lambda_i T_D)/\lambda_i^2 \qquad (A2)$$

$i=1,2,3$ for RaA, RaB, RaC. And for simultaneous counting and sampling,

$$f_i = [\lambda_i T + \exp(-\lambda_i T) - 1]/\lambda_i^2 \qquad (A3)$$

introduce

$$\Delta T = \ln\{\lambda_3\sinh(\lambda_2 t/2)/[\lambda_2\sinh(\lambda_3 t/2)]\}/(\lambda_2-\lambda_3)$$
$$\psi = \{[2\sinh(\lambda_3 t/2)/\lambda_3 t]^{\lambda_2}\cdot[2\sinh(\lambda_2 t/2)/\lambda_2 t]^{-\lambda_3}\}^{1/(\lambda_2-\lambda_3)}$$
$$\zeta = 2\sinh(\lambda_1/2)\exp(-\lambda_1\Delta t)/\lambda_1 t\psi \qquad \text{(A4)}$$

denote $\frac{\lambda_2}{\lambda_2-\lambda_1}\cdot\frac{\lambda_3}{\lambda_3-\lambda_1}$ with w

we can rewrite (A1) into

$$n_A/\psi_s\psi_m = aa'\zeta_s\zeta_m C_A$$
$$n_C/\psi_s\psi_m = (waa\zeta_s\zeta_m + ad')C_A + b'C_B + c'C_C \qquad \text{(A5)}$$

and total counts

$$N_A + N_C = \eta_C vn = [(aa'R + ad')C_A + b'C_B + c'C_C]\psi_s\psi_m\eta_c v$$

coefficients with prime are those corresponding to the effective delay time $T_D' = T_D - \Delta T_s - \Delta T_m$ with

$$f'_i = \exp(-\lambda_i T_D')$$
$$ad' = ac' - aa'w$$
$$R = (\eta_A/\eta_C + w)\zeta_s\zeta_m$$

This helps in expressing the effect of finite t_s into a single ψ and small corrections.

REFERENCES

1 Ji Wanhua, Li Deping. Atomic Energy, 1964(8): 711(in Chinese)

2 Li Deping. Radiation Protection, 1981, 1(3): 1(in Chinese)

AN ELECTRON TRANSPORT THEORY OF CAVITY IONIZATION

Luo Zhengming

(Southwestern Institute of Physics, P. O. Box 15, Leshan, Sichuan, P. R. China)

Zhengming L. An Electron Transport Theory of Cavity Ionization. Radiat. Res. 84, 1-15(1980).

Abstract An electron transport equation is applied to the study of the cavity ionization phenomenon. It has been proved that the effect of the cavity on the energy spectrum of electrons inside this cavity can be attributed to an equivalent electron source uniformly distributed in the cavity. A formula for the energy spectrum of the equivalent electron source is obtained. The deposited energy due to the equivalent electron source in the cavity of the plate chamber has been calculated. The new theory, compared with experimental results, is better than the Spencer-Atitx theory for describing the phenomenon of cavity ionization.

The idea that ionization in the cavity may be applied to estimating energy deposition in the surrounding medium was first proposed by Bragg[1]. A similar idea was again formulated by Gray in his cosmic ray research, and the relationship between the energy deposition of radiation in the medium and ionization in the cavity was found[2,3]. It is generally called the Bragg-Gray principle. Many experiments have shown that the Bragg-Gray principle is more accurate in cavities of greater dimensions for such wall material as graphite, whose atomic number is approximately that of air. However, many experiments, including Gray's own work, have shown that the difference between the prediction of the Bragg-Gray principle and experimental results is appreciable for such wall materials as lead, tin, and copper, whose atomic numbers differ greatly from that of air. In contradiction with the conclusion of the theory, the experiments have shown that specific ionization (i. e., ionization per gram gas in the cavity) regularly varies with the dimension of the cavity[4~6]. This variation is especially apparent in experiments with X and γ rays of lower energy[7]. It is clear that the Bragg-Gray principle cannot fully describe the phenomenon of ionization in the cavity.

Analyzing the discrepancy between the Bragg-Gray principle and ionization experiments with small cavity chambers, Spencer and Attix[8] and Burch[9] published their theoretical work in 1955. They showed that a full analysis of the electron spectrum in the wall ought to take into account accumulation of δ electrons with higher energy. The fundamental assumption of the Bragg-Gray principle has been kept in the Spencer-Attix theory; i. e., the electron spectrum in